

Pygmy resonances in Sn isotopes within a microscopic multiphonon approach

E G Lanza¹, M V Andrés², F Catara¹, Ph Chomaz³ and D Gambacurta¹

¹ I.N.F.N.-Catania and Dipartimento di Fisica e Astronomia, Università di Catania, Via S. Sofia 67, I-95123 Catania, Italy

² Departamento de Física Atomica, Molecular y Nuclear, Universidad de Sevilla, Apdo 1065, E-41080 Sevilla, Spain

³ GANIL (DSM-CEA/IN2P3-CNRS), B.P. 55027, F-14076 Caen Cédex 5, France

E-mail: edoardo.lanza@ct.infn.it

Abstract. We study the pygmy resonances in Sn isotopes within a microscopic multiphonon approach which has been successfully applied to heavy ion reactions in recent years. In the energy region of the pygmy resonances there are a few low lying multiphonon states. The question is whether they may contribute to the observed peak. Calculations show that the inelastic cross sections in the relevant energy region have a considerable increase depending on the isotope and on the kind of Skyrme force used.

1. Introduction

Studies of exotic modes of excitation in nuclei far from the β -stability line are very rich and in the last years have been investigated deeply due to the increase of experimental facilities now running around the world (see Ref. [1] and reference quoted therein). The dipole response has revealed a spreading of strength into the low energy region which is particularly relevant for nuclei with a pronounced neutron skin. This concentration of strength has been attributed to a resonant oscillation of the neutron in excess against an inert core and it is known as Pygmy Dipole Resonance (PDR). Whether this strength is due to a collective mode is still under discussion.

In recent past years we have acquired a skill on the study of multiple giant resonances excitation in heavy ion collisions by means of a microscopic description of the structure of the excited nucleus which includes anharmonicity [2, 3, 4, 5]. Calculations of the inelastic cross section, within a semiclassical coupled channel approach, have revealed the possibilities to excite, in an appreciable way, low lying two-phonon states which lay in the same energy range of the PDR. The motivation of this paper is to try to answer to the question whether these states may contribute to the observed PDR peak. At the same time we would like to investigate the nature of the these low lying dipole states in order to establish whether they can be considered as collective ones.

2. Multiphonon excitations

In this section we will describe, very shortly, the framework within which the calculations for the multiple excitations of giant resonance have been done and whose details can be found in

Refs. [2, 3, 4, 5].

2.1. The model

Great successes have been achieved in the study of excitation processes of heavy nuclei by using semiclassical methods techniques. These methods are based on the assumption that nuclei move on classical trajectories, while the internal degrees of freedom are treated quantum mechanically. The standard approach to study the double excitation of giant resonances implies the use of an internal Hamiltonian which is of harmonic type and an external excitation field which is linear in the phonon creation operators. In our model we have included anharmonicities in the internal Hamiltonian and non-linearities in the external field. These corrections have been included in order to overcome some anomaly in the experimental results.

One of the best microscopic theory to describe collective vibrations in nuclei is the Random Phase Approximation (RPA) whose hamiltonian, at the lowest order of a boson expansion[6], is harmonic in the boson creation operators. The introduction of anharmonicities in the internal Hamiltonian can be achieved by adding to the RPA Hamiltonian the $pppp$, $hhhh$, $ppph$ and $hhhp$ terms which come out by applying a boson mapping procedure to the fermionic Hamiltonian up to second order. So, the boson Hamiltonian now contains terms that mix states with the same number (≥ 2) of phonons and terms which mix states whose phonon numbers differ by one[2, 3, 4, 5].

Our one-phonon basis are chosen from the states resulting from the self-consistent Hartree Fock plus RPA calculations with angular momentum less or equal to 3 and with an appreciable percentage of energy weighting sum rule (EWSR). Then we construct all possible two- and three-phonon states out of them and by diagonalizing the residual interaction in the space of one-, two- and three-phonons states, we obtain the eigenstates of the Hamiltonian, which are mixed states

$$|\Phi_\alpha \rangle = \sum_{\nu} c_{\nu}^{\alpha} |\nu \rangle + \sum_{\nu_1 \nu_2} d_{\nu_1 \nu_2}^{\alpha} |\nu_1 \nu_2 \rangle + \sum_{\nu_1 \nu_2 \nu_3} e_{\nu_1 \nu_2 \nu_3}^{\alpha} |\nu_1 \nu_2 \nu_3 \rangle \quad (1)$$

whose corresponding eigenvalues are not harmonic.

In these semiclassical models the excitation of one of the partners of the collision is due to the mean field of the other. In standard models the excitation operator is of one-body type and it is assumed to be linear in the phonon operators because only terms of ph type are taken into account. Applying the same boson expansion quoted above and taking also the contributions from pp and hh terms, we obtain a non-linear excitation field which depends on time through the relative distance between the two nuclei. Two new terms appear now in the excitation field expression[2, 3, 4]: One connects states with the same number of phonons, while the other allows transitions between states whose number of phonons differs by two.

Both novel aspects may increase the excitation probability of the considered states. By expressing the state of the system in the presence of the excitation operator as a superposition of the $|\Phi_\alpha \rangle$'s, the solution of the time dependent Schrödinger equation is cast into a set of coupled differential equations for the amplitudes which are integrated along the classical relative motion trajectories. For each $|\Phi_\alpha \rangle$ the associated cross section is obtained by integrating the excitation probability over the whole impact parameters range modulated by the transmission coefficient [2, 3, 4].

2.2. Cross sections calculations

Calculations within this framework have been done for various Sn isotopes and with two Skyrme interactions: SGII[7] and SLY4[8]. In all the cases we run a self-consistent HF+RPA code for both interaction, we include all one-phonon states with angular momentum less or equal to 3 and with an EWSR more than 5%. Following the same prescription used previously[2, 4], we

Table 1. RPA one-phonon basis for the nucleus ^{132}Sn and for both SGII and SLY4 interactions. For each state, spin, parity, energy and percentage of the EWSR (isovector for the GDR and the IVGQR and isoscalar for all the other states) are reported.

State	J^π	SGII		SLY4	
		E_{harm} (MeV)	$EWSR$ (%)	E_{harm} (MeV)	$EWSR$ (%)
0_{ll}^+	0^+	11.73	2	11.36	2
GMR	0^+	16.32	85	16.87	86
1_{ll}^-	1^-	9.30	1.1	9.60	1.4
GDR	1^-	13.92	56	13.81	55
1_{hl}^-	1^-	18.34	25	17.75	15
2_{ll}^+	2^+	5.03	11	5.35	11
ISGQR	2^+	13.50	77	14.11	70
IVGQR	2^+	24.76	28	24.03	36
3_{ll}^-	3^-	5.93	27	6.48	26
HEOR	3^-	24.44	32	25.81	30

put together the states in a given small energy interval in such a way to construct a single state at an energy equal to the average value obtained by weighting the energy of the single states by their $B(E\lambda)$ and whose components are obtained with the constraint that it exhausts the fraction of EWSR given by the sum of the EWSR of the states considered. In this way we obtain a reduced set of states which constitute our one-phonon basis. In tables 1 and 2 we show the RPA one-phonon basis for the two isotopes ^{132}Sn and ^{140}Sn . Then we construct all possible two- and three-phonon states out of them and in this space we diagonalize the bosonic Hamiltonian. All the details of the calculations can be found in Ref. [4].

The calculated inelastic cross sections for the Coulomb excitation of ^{132}Sn and ^{140}Sn in the collision with ^{208}Pb at 500 MeV/A are reported in figures 1 and 2. The bars are the cross section for every single state. The full curves are generated by a smoothing procedure using a Lorentzian with a 2 MeV width. In the left (right) part of the figures the results obtained with the SGII (SLY4) interaction are reported. Although we include all the states up to 30 MeV excitation energy, we show the cross sections only in the PDR energy region. We show, for each reaction, the calculations corresponding to two different approximations. The dashed (black) lines are the cross section obtained by taking the harmonic and linear limit. In this case only the basis states (shown in tables 1 and 2) are excited. In the second limit approximation we take into account the anharmonicity and the nonlinearity and the results are shown in the figures with full (red) lines. Several more states are now excited, all of them are not visible in the figure because their individual cross section is below 1 mb. Most of them are states which in the harmonic limit are pure two-phonon components. When the anharmonicities are switched on, they are pushed down and acquire a relatively strong one-phonon component. Therefore the linear term of the field can excite them through such component. In addition there is a contribution also from the other terms of the external field. This behaviour is similar for the two interactions considered here. However, the SLY4 interaction show a difference as far as the anharmonicity is concerned. Such different response will be investigated in a future work.

In order to have a quantitative measure of the effects of the low lying two-phonon states on

Table 2. Same as table 1 but for ^{140}Sn .

State	J^π	SGII		SLY4	
		E_{harm} (MeV)	$EWSR$ (%)	E_{harm} (MeV)	$EWSR$ (%)
GMR	0^+	16.22	82	16.88	79
1_{ll}^-	1^-	7.50	3	7.26	5
GDR	1^-	13.64	46	13.31	54
1_{hl}^-	1^-	17.56	22	17.63	18
2_{ll1}^+	2^+	1.70	3	1.92	2
2_{ll2}^+	2^+	5.78	6	6.37	6
ISGQR	2^+	13.01	76	13.63	74
IVGQR	2^+	24.00	32	24.08	38
3_{ll1}^-	3^-	2.97	9	3.84	9
3_{ll2}^-	3^-	6.24	17	6.82	18
HEOR	3^-	23.93	29	25.29	38

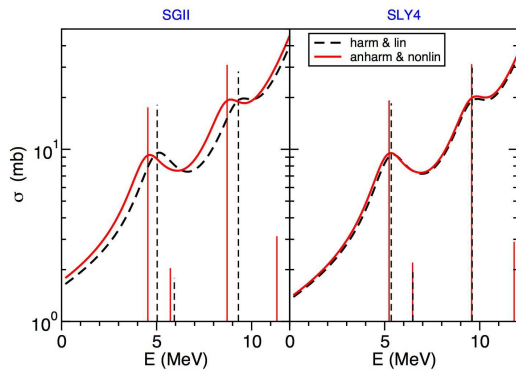


Figure 1. (Color online) Relativistic Coulomb inelastic cross section for $^{132}\text{Sn} + ^{280}\text{Pb}$ at 500 MeV/A with the SGII (left) and SLY4 (right) interactions. The dashed black lines are the cross section obtained in the harmonic and linear approximation. The solid red lines correspond to the anharmonic and nonlinear case.

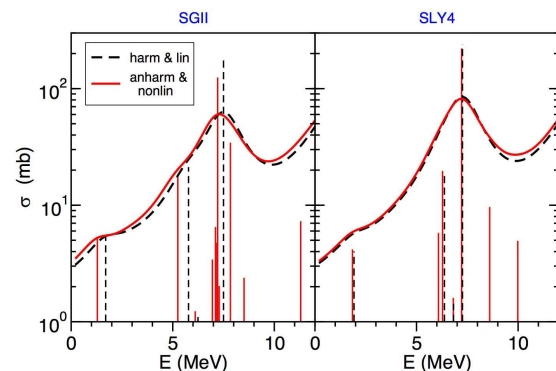


Figure 2. (Color online) Relativistic Coulomb inelastic cross section for $^{140}\text{Sn} + ^{280}\text{Pb}$ at 500 MeV/A with the SGII (left) and SLY4 (right) interactions. The dashed black lines are the cross section obtained in the harmonic and linear approximation. The solid red lines correspond to the anharmonic and nonlinear case.

the inelastic cross section, we have summed the cross section over the energy interval shown in the figures. In table 3 we show the summed cross section for the two reactions considered here: ^{132}Sn , $^{140}\text{Sn} + ^{208}\text{Pb}$ at 500 MeV/A (for both SGII and SLY4 interactions) over the interval 0-12 MeV. The values for the anharmonic and nonlinear case (AH-NL) are sensibly higher than the ones for the harmonic and linear (HL) approximations. The absolute values of the cross section is directly related to the $B(E\lambda)$ values of the low lying 1^- states. The increase is higher for the SGII case: we have 14% increase for the ^{132}Sn isotope and only 5% for ^{140}Sn ; for the

Table 3. Summed inelastic cross sections (in mb) for the systems ^{132}Sn , $^{140}\text{Sn} + ^{208}\text{Pb}$ at 500 MeV/A (for both SGII and SLY4 interactions) over the interval 0-12 MeV. Values for the harmonic and linear case (H-L, second and fourth columns) should be compared with the ones obtained in the anharmonic and non linear calculations (AH-NL, third and fifth columns).

	SGII		SLY4	
	H-L	AH-NL	H-L	AH-NL
^{132}Sn	48.3	55.0	50.2	55.8
^{140}Sn	203.3	213.6	264.5	269.4

SLY4 interaction these increases are 11% for ^{132}Sn and only 2% for ^{140}Sn . We can certainly state that the inclusion of multiphonon states in the study of the PDR excitation has revealed to be important at least when the SGII interaction is used. The minor contribution obtained with the SLY4 interaction should be related to the weaker anharmonicity found in this case: An aspect which should be investigated in a future work.

3. The low lying 1^- states

In this section we would like to study the nature of the low lying 1^- states, in particular we would like to address the question whether or not the dipole strength at low energy corresponds to a collective mode. Previous investigations within the quasiparticle RPA have found that the peak associated to the PDR is due to a neutron strong single p-h configuration [9]. On the other hand, calculations done within the relativistic RPA [10] have got results which are at variance with those quoted above. The RPA dipole strength distribution for some Sn isotopes are reported in figure 3. The bars correspond to the RPA calculations while the full lines are generated by a smoothing procedure using a Lorentzian with a 1 MeV width. The figure shows clearly that when the neutron excess increases more strength develops or moves at low energy acquiring for the ^{140}Sn a considerable strength below 10 MeV. This result is similar for both interactions.

Another effect already underlined in previous work [11] and related to the increase of the neutron skin is a rather strong isospin mixing which develops in states of higher multipolarities. As an example we show in figure 4 the isoscalar (upper part) and isovector (lower part) RPA quadrupole strength distribution for ^{100}Sn where we can clearly distinguish two pure isoscalar states and an isovector strength concentrated around 27 MeV which can be assigned to the isovector GQR. As far as the neutron skin increases some strength of the isovector part moves to lower energy generating states with a strong isospin mixing. This general behaviour has been found also for octupole states and it is independent of the interaction used as far as our calculations are concerned.

The important question is how much collective are the dipole states whose strength lay at low energy. One measure of the collectivity is the number of p-h component entering in the RPA wave function with an appreciable weight [9, 10]. In microscopic calculations this can be analyzed in more details by defining the quantity

$$A_{ph} = |X_{ph}^\nu|^2 - |Y_{ph}^\nu|^2 \quad (2)$$

in terms of the X and Y RPA's amplitudes, with the normalization condition

$$\sum_{ph} A_{ph} = 1 \quad (3)$$

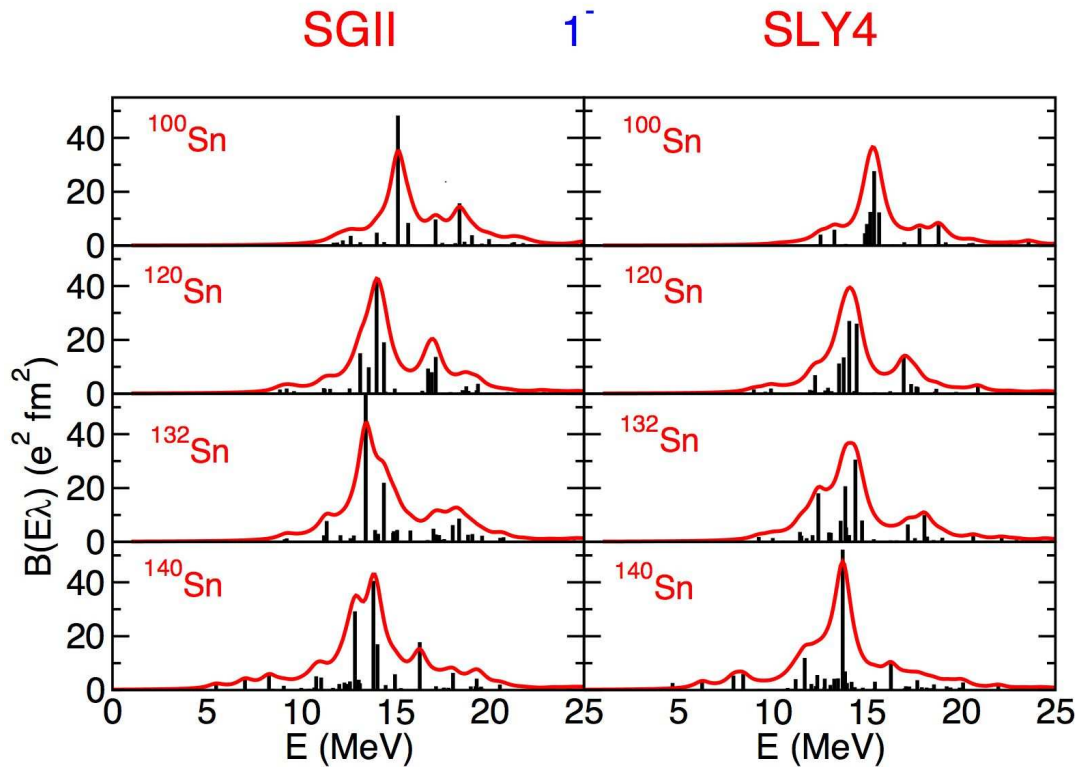


Figure 3. (Color online) Strength distributions for dipole states for tin isotopes calculated with the SGII and SLY4 interactions, left and right columns, respectively. The solid curves are obtained by adopting a smoothing procedure (see text).

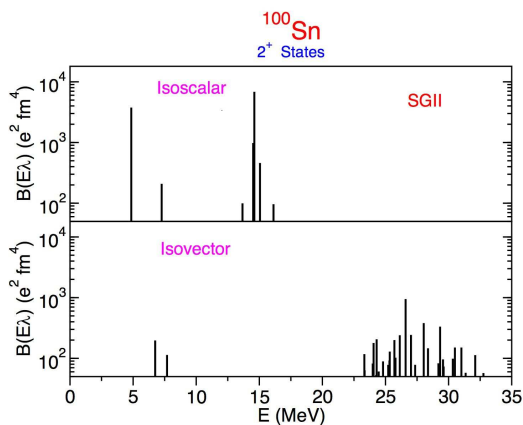


Figure 4. Isoscalar (upper part) and isovector (lower part) RPA strength distributions for quadrupole states for ^{100}Sn isotope calculated with the SGII interaction.

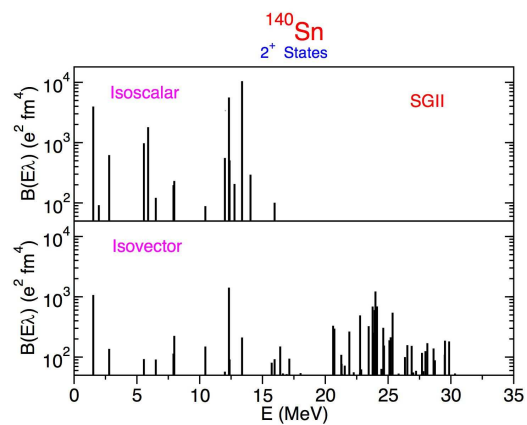


Figure 5. Isoscalar (upper part) and isovector (lower part) RPA strength distributions for quadrupole states for ^{140}Sn isotope calculated with the SGII interaction.

In table 4 we show for each p-h configuration its contribution, in percentage, to the formation of the low lying 1^- states shown in table 1. Only the configurations contributing more than 1% are shown. Note that the major contribution comes from the neutron skin. Indeed, the

Table 4. Particle-hole configurations which give the major contribution for the two dipole low-lying states (shown in table 1) for the nucleus ^{132}Sn and for the SGII and SLY4 interactions. For each p-h configuration the contribution to the norm of the state and the partial contribution to the reduced transition amplitude (in e fm units) are reported. The superscripts π , ν refer to the proton and neutron states, respectively.

SGII (E=9.3 MeV)		SLY4 (E=9.6 MeV)	
p-h conf.	A_{ph}	p-h conf.	A_{ph}
$(2p_{3/2}, 3s_{1/2})^\pi$	1.0%	$(1f_{5/2}, 1g_{7/2})^\pi$	1.1%
$(2p_{3/2}, 2d_{5/2})^\pi$	7.0%	$(2p_{3/2}, 2d_{5/2})^\pi$	1.8%
$(2p_{1/2}, 3s_{1/2})^\pi$	2.8%	$(1g_{9/2}, 1h_{11/2})^\pi$	5.6%
$(1g_{9/2}, 1h_{11/2})^\pi$	12.5%	$(1g_{7/2}, 1h_{9/2})^\nu$	1.9%
$(1g_{7/2}, 1h_{9/2})^\nu$	2.1%	$(2d_{3/2}, 3p_{1/2})^\nu$	30.0%
$(2d_{5/2}, 2f_{7/2})^\nu$	1.6%	$(2d_{3/2}, 2f_{5/2})^\nu$	41.8%
$(2d_{3/2}, 3p_{1/2})^\nu$	13.7%	$(3s_{1/2}, 3p_{3/2})^\nu$	6.1%
$(2d_{3/2}, 2f_{5/2})^\nu$	8.6%	$(1h_{11/2}, 1i_{13/2})^\nu$	7.1%
$(3s_{1/2}, 3p_{3/2})^\nu$	20.9%		
$(3s_{1/2}, 3p_{1/2})^\nu$	14.2%		
$(1h_{11/2}, 1i_{13/2})^\nu$	12.2%		

neutron p-h configurations contribute for 73% to the formation of the state, in the case of SGII interaction, and for 87% for the state obtained with the SLY4 interaction. For both cases our result is very similar to the one obtained in Ref. [10] where a relativistic RPA has been used for the study of the pygmy resonance. In fact, also in our case several p-h configurations contribute with an appreciable weight. A more complete analysis should also take into account the degree of coherence of such contributions. That is to say, one has to look also how the p-h contributions sum up to give the final reduced transition probability $B(E\lambda)$. Such analysis has been done in Ref. [12] and it shows how the criterion described above, based only on the magnitude of the A_{ph} , can be misleading. In fact, looking to the construction of the reduced transition probability we found, for the low lying dipole states, strong cancellations leading to a small value for the $B(E1)$ compared with the GDR one. That the nature of these dipole states is qualitatively different from the high lying ones is illustrated in figure 6 where the proton, neutron, isoscalar and isovector transition densities for the two states, calculated with the SGII interaction, are reported. The behaviour for the low-lying state is similar to what has been found for other nuclei with neutron excess[11, 10, 9]: The proton and neutron densities in the interior region are not out of phase; in the interior the isoscalar transition density dominates over the isovector one; in the surface region only the neutrons give a contribution to both isoscalar and isovector transition densities. For the GDR and the 1_{hl}^- cases we find the expected radial dependence for a collective isovector state: the proton and neutron transition densities oscillate out of phase; the isovector part is much larger than the isoscalar one; the latter has a node in the interior of the nucleus which produce a zero result, when integrated over the radial distance, for isoscalar $B(E1)$.

4. Summary

In this work we have extended the study of multiphonon excitations in heavy ion collisions to the case of the pygmy resonances. Indeed, we have found that a few multiphonon states, lying

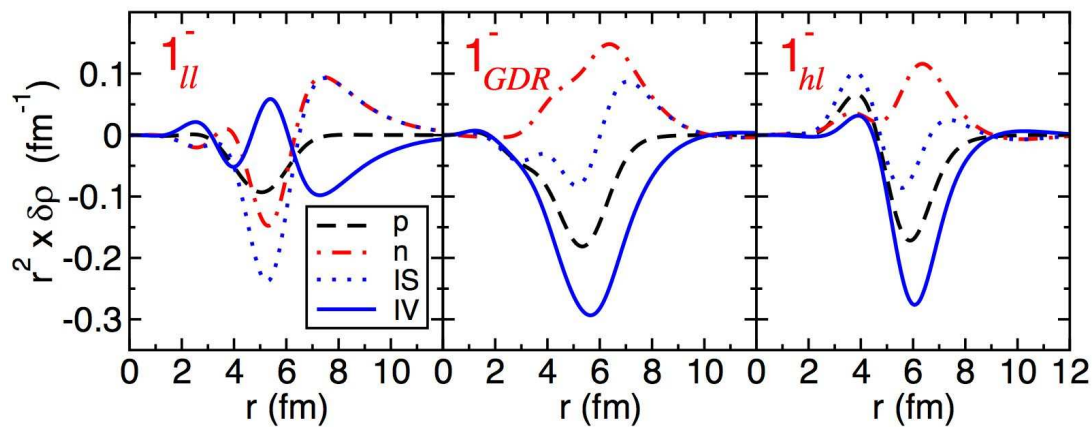


Figure 6. (Color online) Transition densities for the low-lying dipole state, the GDR and the 1^-_{hl} for the ^{140}Sn isotope calculated with the SGII interaction. We show the proton, neutron, isoscalar and isovector parts (as indicated in the legend).

in the PDR energy region, are excited in the collision process with a strong probability. Thus, they may contribute to the observed PDR peak. We start from a microscopic approach based on RPA which is extended by the introduction of anharmonicities generated by the coupling of multiphonon states. The inelastic cross sections are calculated by solving semiclassical coupled channel equations, where the external field has been implemented by taking into account non linearities. The calculations have been done for two different Skyrme interaction (SGII and SLY4) and for the reactions $^A\text{Sn} + ^{280}\text{Pb}$ at 500 MeV/A. We found an increase of the cross section in the low lying PDR energy region which is mainly due to the excitation of several states whose population is strongly suppressed by selection rules when anharmonicities and non-linearities are neglected. In general, the SLY4 interaction produces a smaller anharmonicity which is then reflected in a lower increase of the cross section in the PDR region. On the contrary, the results obtained with the SGII show the importance of anharmonicities and non linearities for the study of the PDR.

References

- [1] Paar N, Vretenar D, Khan E and Colò G 2007 *Rep. Prog. Phys.* **70** 691
- [2] Lanza E G, Andrés M V, Catara F, Chomaz Ph and Volpe C 1997 *Nucl. Phys. A* **613** 445; 1998 *Nucl. Phys. A* **636** 452; 1999 *Nucl. Phys. A* **654** 792c
- [3] Andrés M V, Catara F, Lanza E G, Chomaz Ph, Fallot M and Scarpaci J A 2001 *Phys. Rev. C* **65** 014608
- [4] Lanza E G, Andrés M V, Catara F, Chomaz Ph, Fallot M and Scarpaci J A 2006 *Phys. Rev. C* **74** 064614
- [5] Fallot M, Chomaz Ph, Andrés M V, Catara F, Lanza E G and Scarpaci J A 2003 *Nucl. Phys. A* **729** 699
- [6] Hage-Hassan M and Lambert M 1972 *Nucl. Phys. A* **188** 545
- [7] Van Giai N and Sagawa H 1981 *Phys. Lett.* **106** B 379; Van Giai N and Sagawa H 1981 *Nucl. Phys. A* **371** 1
- [8] Chabanat E, Bonche P, Haensel P, Meyer J and Schaeffer R 1998 *Nucl. Phys. A* **635** 231
- [9] Coló G and Bortignon P F 2001 *Nucl. Phys. A* **696** 427; Sarchi D, Bortignon P F and Coló G 2007 *Phys. Lett. B* **601** 27
- [10] Vretenar D, Paar N, Ring P and Lalazissis G A 2001 *Nucl. Phys. A* **692** 496; Litvinova E, Ring P and Vretenar D 2007 *Phys. Lett. B* **647** 111
- [11] Catara F, Lanza E G, Nagarajan M A and Vitturi A 1997 *Nucl. Phys. A* **614** 86; 1997 *Nucl. Phys. A* **624** 449
- [12] Lanza E G, Andrés M V, Catara F, Chomaz Ph, and Gambacurta D to be published in *Phys. Rev. C*